

Article

Hydroxyapatite Precipitation and Accumulation in Granules and Its Effects on Activity and Stability of Partial Nitrifying Granules at Moderate and High Temperatures

Yong-Qiang Liu * and Simone Cinquepalmi

Faculty of Engineering and Physical Sciences, University of Southampton, Southampton SO17 1BJ, UK; S.Cinquepalmi@soton.ac.uk

* Correspondence: Y.Liu@soton.ac.uk; Tel.: +44-02380592843

Abstract: Precipitation and accumulation of calcium phosphate in granular sludge has attracted research attention recently for phosphate removal and recovery from wastewater. This study investigated calcium phosphate accumulation from granulation stage to steady state by forming heterotrophic granules at different COD/N ratios at 21 and 32 °C, respectively, followed by the transformation of heterotrophic granules to partial nitrifying granules. It was found that mature granules accumulated around 60–80% minerals in granules, much higher than young granules with only around 30% ash contents. In addition, high temperature promoted co-precipitation of hydroxyapatite and calcite in granules with more calcite than hydroxyapatite and only 4.1% P content, while mainly hydroxyapatite was accumulated at the moderate temperature with 7.7% P content. The accumulation of minerals in granules at the high temperature with 75–80% ash content also led to the disintegration and instability of granules. Specific ammonium oxidation rates were reduced, as well, from day 58 to day 121 at both temperatures due to increased mineral contents. These results are meaningful to control or manipulate granular sludge for phosphorus removal and recovery by forming and accumulating hydroxyapatite in granules, as well as for the maintenance of microbial activities of granules.

Keywords: nitrifying granules; hydroxyapatite; calcite; stability; microbial activity; phosphorus removal and recovery



Citation: Liu, Y.-Q.; Cinquepalmi, S. Hydroxyapatite Precipitation and Accumulation in Granules and Its Effects on Activity and Stability of Partial Nitrifying Granules at Moderate and High Temperatures. *Processes* **2021**, *9*, 1710. <https://doi.org/10.3390/pr9101710>

Academic Editor: Maria Jose Martin de Vidales

Received: 19 July 2021

Accepted: 15 September 2021

Published: 24 September 2021

Publisher's Note: MDPI stays neutral with regard to jurisdictional claims in published maps and institutional affiliations.



Copyright: © 2021 by the authors. Licensee MDPI, Basel, Switzerland. This article is an open access article distributed under the terms and conditions of the Creative Commons Attribution (CC BY) license (<https://creativecommons.org/licenses/by/4.0/>).

1. Introduction

Aerobic granular sludge is a promising technology to replace suspended sludge for wastewater treatment. Basically, granular sludge is a kind of self-immobilized biofilm without carriers, which was developed in the 1980s in Upflow Anaerobic Sludge Blanket (UASB) systems for anaerobic wastewater treatment, and in the 2000s in Sequential Batch Reactor (SBR) systems for aerobic wastewater treatment. Compared with suspended sludge, granular sludge possesses a compact structure and large size, which is believed to be favorable to inorganic precipitation and accumulation in granules. High inorganic content in aerobic granules, anaerobic granules, and ANAMMOX granules under some operational conditions have been widely observed and reported [1–3]. Reactor operation mode might affect inorganic mineral accumulation in granules. It was found that, after the operation mode was changed from sequential batch to continuous, the ash content of aerobic granules increased from 20 to 84% with inorganic minerals identified by XRD analysis as CaCO₃, although Ca²⁺ concentration in wastewater as low as 19 mg L⁻¹ [4]. Since heavy and large granules are more easily retained in reactors, particularly at the bottom of the reactors, the ash content of ANAMMOX granules at the reactor bottom was 60%, while it was only 10% at the reactor top [5]. Juang et al. [6] hypothesized that calcium and/or iron precipitates in the granule interior substantially enhanced the structural stability of aerobic granules under continuous operation mode, while Liu et al. [7] reported a significantly reduced microbial activity of biomass under continuous operation mode with

the excessive precipitation of CaCO_3 , although granules maintained excellent structural stability. From these studies, it looks as if the inorganic precipitation and accumulation in granules are conducive to the structural stability of granular sludge. Furthermore, it was reported that the granulation period was shortened by adding extra metal ions, such as Ca^{2+} [8] Mg^{2+} , Al^{3+} [9], Fe^{3+} [10], and Mn^{2+} . It was speculated that metal ions could form metal precipitates which could become the nucleus for bacteria to attach to form granules with a similar mechanism for biofilm growth. This theory seems to be partially supported by the phenomenon that inorganic precipitates were mostly found in the core of granules [11,12]. However, so far, there are no reports about the comparison between the newly formed granules and mature granules regarding the spatial distribution of inorganic precipitates to fully validate biofilm growth theory.

Biologically induced precipitation in granules is another mechanism proposed to explain mineral precipitates in granules [3,13]. It was believed that a three-dimensional compact structure working together with biological activities inside, such as nitrification, denitrification, and biological phosphorus removal, could change the chemical environment in granules, thus benefiting metal precipitation [13]. Although the mechanism of mineral precipitation in granules is unclear, there is no doubt that divalent or trivalent metal ions could accelerate granulation, increase granule compactness, and decrease SVI. The long-term stability of granules with high mineral precipitates is unclear. Reduced microbial activities of granules with high mineral precipitates have been reported [4,14–16], but it is unclear how high mineral precipitate contents affect microbial activities of nitrifying bacteria in granules with varied pH in SBR cycles.

Temperature is another factor that needs to be investigated for its effect on precipitation in granules because temperature affects biomass growth rate, nitrification rate, precipitation speed, the solubility of mineral precipitates, and the stability of granules. Aerobic granulation, granule stability, COD, N, and P removal could be achieved from a wide range of temperatures, i.e., from 8 °C to 50 °C, although sludge characteristics and treatment performance could be different [17,18]. With the development and implementation of ANAMMOX for nitrogen removal, partial nitrification under high temperatures, such as 30–35 °C, was demanded before ANAMMOX. How mineral precipitates in nitrifying granules at different temperatures affect granule stability and microbial activities of nitrifying bacteria is still unknown.

Furthermore, in practice, it is less likely to dose extra Ca^{2+} , Mg^{2+} , Al^{3+} , or Fe^{3+} as research was done in labs to stimulate granulation or maintain granule stability because it involves the extra cost of chemicals, handling, and storage. However, in different regions, water hardness levels are different with a wide range of Ca^{2+} and Mg^{2+} concentrations. For example, in the east and south of England, Ca^{2+} concentration in water reaching as high as 150 mg L^{-1} and 50–100 mg L^{-1} of Ca^{2+} in water is very common. How a high water hardness level with a high Ca^{2+} concentration affects mineral precipitation in granules and reactor performance is important for the implementation of granular sludge technology in these regions.

Thus, this study aims to investigate mineral precipitates and their effects on the formation, activity, and stability of nitrifying granules at moderate and high temperatures in regions with a high water hardness level. It is expected that this study would provide some practical guidance on the operation of nitrifying granule reactors. Meanwhile, it could shed light on the possible mechanisms involved in mineral precipitation and accumulation in granules, as well as granule stability.

2. Materials and Methods

2.1. Reactors Operation and Inoculum

Four Perspex columns (R1, R2, R3, and R4), each with a working volume of 2.6 L and a column height to diameter ratio of 20 (Ø 60 mm), were operated sequentially with a cycle time of 4 h. The cycle consisted of 10-min feeding, 227–199 min aeration, 2–30 min settling time, and 1-min discharging. The effluent was discharged from the middle port of the

reactors, corresponding to a volumetric exchange ratio of 50%. The air was provided from the reactor bottom with a flow rate of 5 L min^{-1} , corresponding to a superficial velocity of 3.0 cm s^{-1} .

The reactors were started up at two different temperatures, i.e., ambient temperature at $21 \text{ }^\circ\text{C}$ and high temperature at $32 \text{ }^\circ\text{C}$, by inoculating 3.2 g L^{-1} activated sludge from Portswood Wastewater Treatment Plant, Southampton, UK, which was only for COD removal without nitrification capability. The reactor operation was divided into four phases: (i) In phase 1, the inoculated activated sludge was converted into heterotrophic granules by providing high OLR and short settling time; (ii) in phase 2, the nitrifying bacteria were enriched within heterotrophic granules by decreasing COD/N ratio until no organic carbon was provided; (iii) in phase 3, NH_4^+ concentration was quickly elevated to speed-up the AOBs enrichment; and, (iv) in phase 4, long-term stability of nitrification systems was tested. The specific operational conditions for four reactors are listed in Table 1.

Table 1. Specific operational conditions of four reactors for granulation and nitrification.

		Units	R1	R2	R3	R4
	Temperature	$^\circ\text{C}$	21 ± 3	32 ± 2	21 ± 3	32 ± 2
Phase 1 (0–21)	COD	mg L^{-1}	1000	1000	1000	1000
	NH_4^+	mg N L^{-1}	50	50	200	200
	COD/N		20	20	5	5
Phase 2 (22–37/49 ^a)	COD	mg L^{-1}	1000 to 0	1000 to 0	1000 to 0	1000 to 0
	NH_4^+	mg N L^{-1}	50 to 400	50 to 850	200 to 150	200 to 750
Phase 3 (38/50 ^a –107)	NH_4^+	mg N L^{-1}	Varied influent ammonium concentration ^b			
Phase 4 (108–171)	NH_4^+	mg N L^{-1}	500	65	650	850

^a Phase 2 lasted until day 37 for R2 and R4 and until day 49 for R1 and R3. ^b The influent NH_4^+ concentrations to 4 reactors were varied to ensure more than 90% ammonium-nitrogen removal until the values in phase 4 (R2 collapsed so influent NH_4^+ concentration was reduced).

By designing experiments for the operation of 4 reactors under conditions listed in Table 1, we can compare granulation and stability of nitrifying granules for (i) effects of COD/N ratios (i.e., 20 and 5) on heterotrophic granulation at ambient temperature, i.e., $21 \pm 3 \text{ }^\circ\text{C}$, between R1 and R3; (ii) effects of COD/N ratios (i.e., 20 and 5) on heterotrophic granulation at high temperature, i.e., $32 \pm 2 \text{ }^\circ\text{C}$, between R2 and R4; (iii) effects of temperature (i.e., $21 \pm 3 \text{ }^\circ\text{C}$ and $32 \pm 2 \text{ }^\circ\text{C}$) on heterotrophic granulation at COD/N of 20 between R1 and R2; and (iv) effects of temperature (i.e., $21 \pm 3 \text{ }^\circ\text{C}$ and $32 \pm 2 \text{ }^\circ\text{C}$) on heterotrophic granulation at COD/N of 5 between R3 and R4. In addition, once heterotrophic granules were completely converted into nitrifying granules, we can compare (i) activity and the long-term stability of nitrifying granules at two different temperatures, between R3 and R4 or between R1 and R2; and (ii) effects of initial COD/N ratios on the long-term stability of nitrifying granules between R1 and R3 or between R2 and R4.

2.2. Medium

Synthetic wastewater was prepared with tap water, in which sodium acetate, ammonium sulphate, and mono-potassium phosphate were added as carbon, nitrogen, and phosphorous sources, respectively, with COD, NH_4^+ -N concentrations, as shown in Table 1, and phosphorous concentration as $15 \text{ mg PO}_4^{3-}\text{-P L}^{-1}$. In phase 2, for nitrifying bacteria enrichment, the organic carbon concentration was reduced stepwise, along with a concurrent increase in ammonium and NaHCO_3 concentrations with a ratio of $1 \text{ mg NH}_4^+\text{-N}$ to 14 mg NaHCO_3 . The bicarbonate was used as the inorganic carbon source for autotrophic nitrifying bacteria, as well as a buffer for pH. In phase 4, the ammonium concentrations were kept constant since the nitrifying granules had reached the process stability.

Apart from carbon, nitrogen and phosphorus sources, micronutrients were added as (per liter prepared): 25 mg $\text{CaCl}_2 \cdot 2\text{H}_2\text{O}$, 20 mg $\text{MgSO}_4 \cdot 7\text{H}_2\text{O}$, and 10 mg $\text{FeSO}_4 \cdot 7\text{H}_2\text{O}$. The trace elements were (per liter prepared): 0.12 mg $\text{MnCl}_2 \cdot 4\text{H}_2\text{O}$, 0.12 mg $\text{ZnSO}_4 \cdot 7\text{H}_2\text{O}$, 0.03 mg $\text{CuSO}_4 \cdot 5\text{H}_2\text{O}$, 0.05 mg $(\text{NH}_4)_6\text{Mo}_7\text{O}_{24} \cdot 4\text{H}_2\text{O}$, 0.1 mg $\text{CoCl}_2 \cdot 6\text{H}_2\text{O}$, 0.1 mg $\text{NiCl}_2 \cdot 6\text{H}_2\text{O}$, 0.05 mg $\text{AlCl}_3 \cdot 6\text{H}_2\text{O}$, and 0.05 mg H_3BO_3 . From phase 3 (day 47), both CaCl_2 and MgSO_4 were removed from feedstock after excessive inorganic precipitation, and accumulation within the granules was observed. The synthetic wastewater pH was not adjusted, but it was around 7.2–7.4.

2.3. Analytical Methods

COD, mixed liquor suspended solids (MLSS), mixed liquor volatile suspended solids (MLVSS), sludge volume index (SVI), and ash content were measured in accordance with standard methods [19]. For the measurement of SVI_{15} , the settled sludge volume was recorded after 5-min settling in a 100-mL graduated cylinder, as opposed to 30 min for SVI_{30} [20]. After granules formed, the density method used by Beun et al. [21] was employed to measure MLSS due to difficulty in homogenous sampling. Ammonium was measured spectrophotometrically by following the procedure in accordance with that described in the manual BSI [22], using the UV-Visible spectrophotometer Cecil 3000 series (Cecil Instruments Ltd., Cambridge, UK). The pH in the reactors (during aeration), and from the effluent, was daily monitored by using a bench pH-meter (Mettler Toledo, Columbus, OH, USA).

Anions (NO_2^- , NO_3^- , PO_4^{3-}) and cations (Ca^{2+} and Na^+) were measured by the ionic chromatographer 882 Compact IC plus (Metrohm, Switzerland). For the measurement of anions, a Metrosep A Supp 5-150/4.0 column was used with the eluent containing 1 mM NaHCO_3 and 3.2 mM Na_2CO_3 . For the measurement of cations, a Metrosep C4 250/4.0 column was used with the eluent containing 1.7 mM HNO_3 and 0.7 mM $\text{C}_7\text{H}_5\text{NO}_4$ (dipicolinic acid or Pyridin-2,6-dicarboxylic acid).

The morphologies of granule external surface and internal parts were observed by using the Quanta 250 scanning electron microscopy (SEM) (FEI, Hillsboro, OR, USA). Representative granules were halved and fixed overnight with a solution of 3% glutaraldehyde + 4% formaldehyde in 0.1 M PIPES buffer with a pH of 7.2. Then, the specimens were washed twice with each for 10 min by 0.1 M PIPES buffer with a pH of 7.2, followed by a series of dehydration steps of 10-min washes with ethanol 30%, 50%, 70%, and 95%, respectively. After these, two rinses with absolute ethanol, lasting 20 min each, were conducted. The granules samples were then dried by a Balzers CPD 030 Critical Point Drier, before being carbon coated by a high-resolution sputter and high vacuum carbon coater (Quorum, Q150T ES, West Sussex, UK) for morphology observation. In addition, the energy dispersive X-ray spectroscopy (EDX) coupled with SEM (EDAX, Mahwah, NJ, USA) was used to qualitatively analyze the chemical elements present in the granules.

Crystals in granules were analyzed by XRD (Bruker D2 phaser, Bruker AXS Gmgh, Karlsruhe, Germany). The granule samples were first washed thoroughly with deionized water to remove any soluble chemicals from the feedstock, and then it was kept at -20°C overnight before being freeze-dried (lyophilized). Before XRD analysis, the dry granules were ground into a fine powder.

The elemental composition of granules was analyzed quantitatively by using a multi collector inductively coupled plasma (ICP) emission spectrometer (X-SERIES 2 ICP-MS, Thermo Fisher Scientific, Bremen, Germany). Before the analysis, the samples were dried at 105°C overnight and then ground into powder. Fifty milligrams of it was digested by adding 2 mL of aqua regia (a 1:3 mixture of 68% nitric acid and 36% hydrochloric acid) and 0.5 mL perchloric acid (68%) in a Teflon digestion vessel on a hotplate (150°C) overnight. After the digestion, 10 mL of concentrated HCl (36%) was added to the completely dry samples. After this solution went dry by evaporating the acid, 3% nitric acid was added to the samples for the analysis by ICP-MS. The data were processed using Plasmalab software.

3. Results and Discussion

3.1. Formation of Heterotrophic Granules with Different COD/N Ratios at Different Temperatures

Temperature effects on granulation were studied at two different influent COD/N ratios, i.e., 5 and 20. It was found that temperature effects at COD/N ratio of 5 were the same as that at COD/N ratio of 20. Thus, only the results of temperature effects on granulation at COD/N ratio of 5 (i.e., the comparison between R3 and R4) are presented in Figure 1. It can be seen that SVI_5 increased sharply in both reactors in the first 3 days and then decreased quickly to less than 100 mL g^{-1} after day 7. This phenomenon is in agreement with those reported by Liu et al. [23] and Liu et al. [24], indicating a typical change of SVI_5 for fast granulation. Once SVI reduced to less than 100 mL g^{-1} , the average sludge size started to increase quickly (Figure 1d), along with the decrease in sludge volume percentage with particle size smaller than $200 \mu\text{m}$ (Figure 1c). Although SVI_5 in both reactors is similar, sludge size increased more quickly in R3 at 21°C (Figure 1d), resulting in a higher biomass concentration in R3 (Figure 1b). On day 21, MLVSS in R3 at 21°C reached 4.6 g L^{-1} , while it was 3.0 g L^{-1} in R4 at 32°C . Based on the definition of granulation by Liu and Tay [25] that sludge volume percentage with particle size smaller than $200 \mu\text{m}$ below 50% represents the formation of granule dominant sludge, granular sludge formed on day 9 in R3 at 21°C , while this occurred on day 11 in R4 at 32°C . Thus, it can be said that granulation speeds at two different temperatures are almost the same, although moderate temperature seems slightly better than high temperature. It was reported that the time needed for total granule formation at 8°C approximated twice the time that is normally needed at 20°C [17], while there was no difference when granules were formed at 30°C and 40°C [18]. From these literature reports and our own results presented here, it could be reasoned that temperature range from 20 to 40°C does not affect granulation speed.

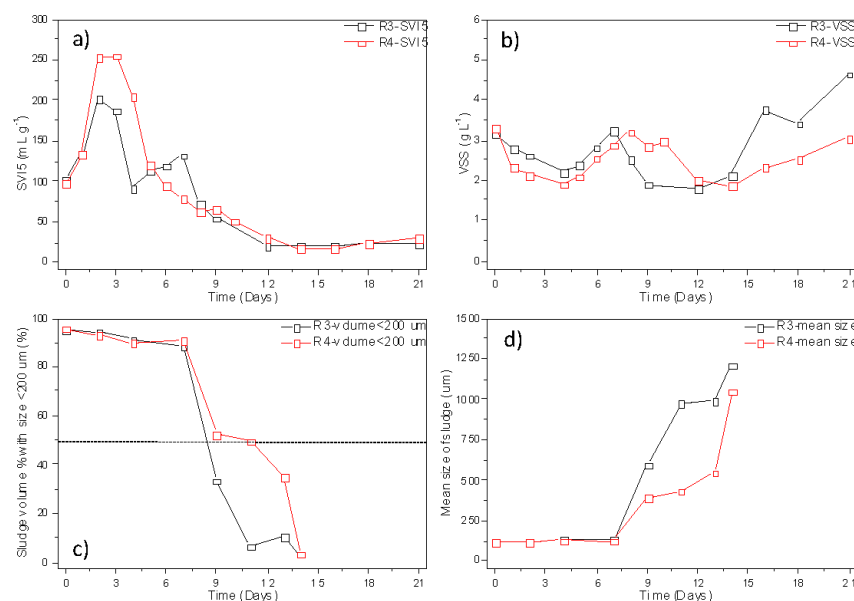


Figure 1. Profiles of SVI_5 (a), MLVSS (b), sludge volume percentage with a size smaller than $200 \mu\text{m}$ (c), and sludge mean size (d) over the time during phase 1 in R3 (21°C) and R4 (32°C) at COD/N of 5 with $\text{NH}_4^+\text{-N}$ concentration of 200 mg L^{-1} .

Figure 2 shows the effects of COD/N ratios on granulation at 32°C , which is the same with those at 21°C (data not shown). As in Figure 1, with the effects of temperature on granulation, SVI_5 in both reactors (i.e., R2 and R4) had the same changing patterns (Figure 2a), but sludge size and biomass concentration showed a slight difference after day 13. Based on the definition of granule dominant sludge mentioned above, granular sludge formed on day 11 in R4 with $200 \text{ mg NH}_4^+\text{-N L}^{-1}$, while on day 13 in R2 with $50 \text{ mg NH}_4^+\text{-N L}^{-1}$.

Because of slightly faster granulation, R4 achieved higher biomass accumulation with a concentration of $3.0 \text{ g MLVSS L}^{-1}$ on day 21, whereas it was $1.8 \text{ g MLVSS L}^{-1}$ in R2. The results suggested that granulation speed was not affected too much by influent ammonium concentration, although it seems that higher ammonium concentration was slightly better. This result is different from that reported by Yang et al. [26] that initial ammonium concentration of 200 mg L^{-1} inhibited granulation, while granules formed when COD/N ratios were above 6. The key difference between this study and Yang et al., in 2004, is that we employed a short settling time, while 20-min settling time was used by Yang et al. [26]

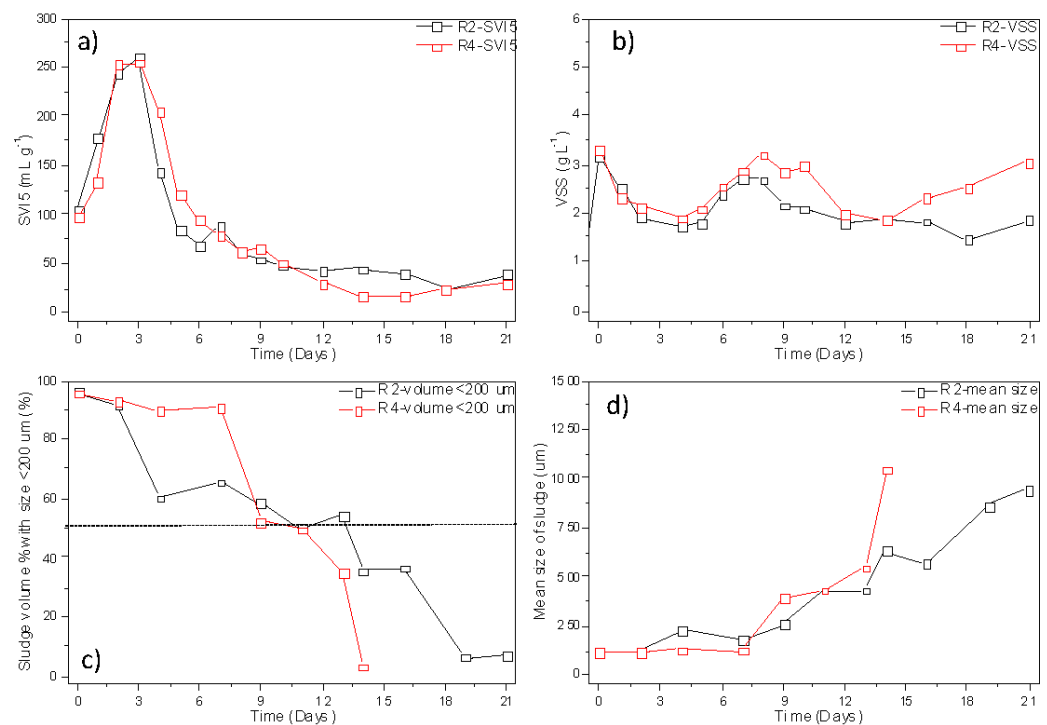


Figure 2. Profiles of SVI₅ (a), MLVSS (b), sludge volume percentages with a size smaller than $200 \mu\text{m}$ (c), and sludge mean size (d) over the time during phase 1 in R2 (with COD/N of 20 and $50 \text{ mg NH}_4^+\text{-N L}^{-1}$) and R4 (with COD/N of 5 and $200 \text{ mg NH}_4^+\text{-N L}^{-1}$) at the operational temperature of $32 \text{ }^\circ\text{C}$.

From Figures 1 and 2, it could be concluded that, as long as the strong hydraulic selective pressure, such as short settling time, was employed to start up granular sludge reactors quickly [27,28], COD/N ratios and temperature have only negligible effects on granulation. This is meaningful for the start-up of the granular sludge reactors under different conditions.

3.2. Mineral Accumulation in Nitrifying Granules Converted from Heterotrophic Granules at Different Temperatures and Minerals Effects on Granules' Long-Term Stability

As shown in Figure 3, the sludge in four reactors showed excellent settleability with SVI₅ lower than 70 mL g^{-1} after 1-week operation, and less than 40 mL g^{-1} , except for R2 after granulation. At the same time, the ash content in sludge increased slightly and slowly from an average value of 18% on day 0 to 19–35% in 4 reactors on day 21, i.e., the end of phase 1 for granulation (Figure 3a), indicating granulation might promote ash accumulation in granules due to the retention of granular sludge. Once granules became dominant with granule percentage higher than 95%, ash contents of granules increased steeply in phase 2, resulting in dense granules with SVI₅ of 14, 5, 23, and 8 mL g^{-1} , respectively, on day 59 (Figure 3b). The comparison between day 21 and day 59 demonstrates that mature granules had much higher ash contents compared with young granules which were just formed. This might be related to granule retention time, and a longer granule retention

time allows more mineral accumulation in granules. A similar high ash accumulation within aerobic granules coupled with such low SVI_5 was also described by other research in literature [7].

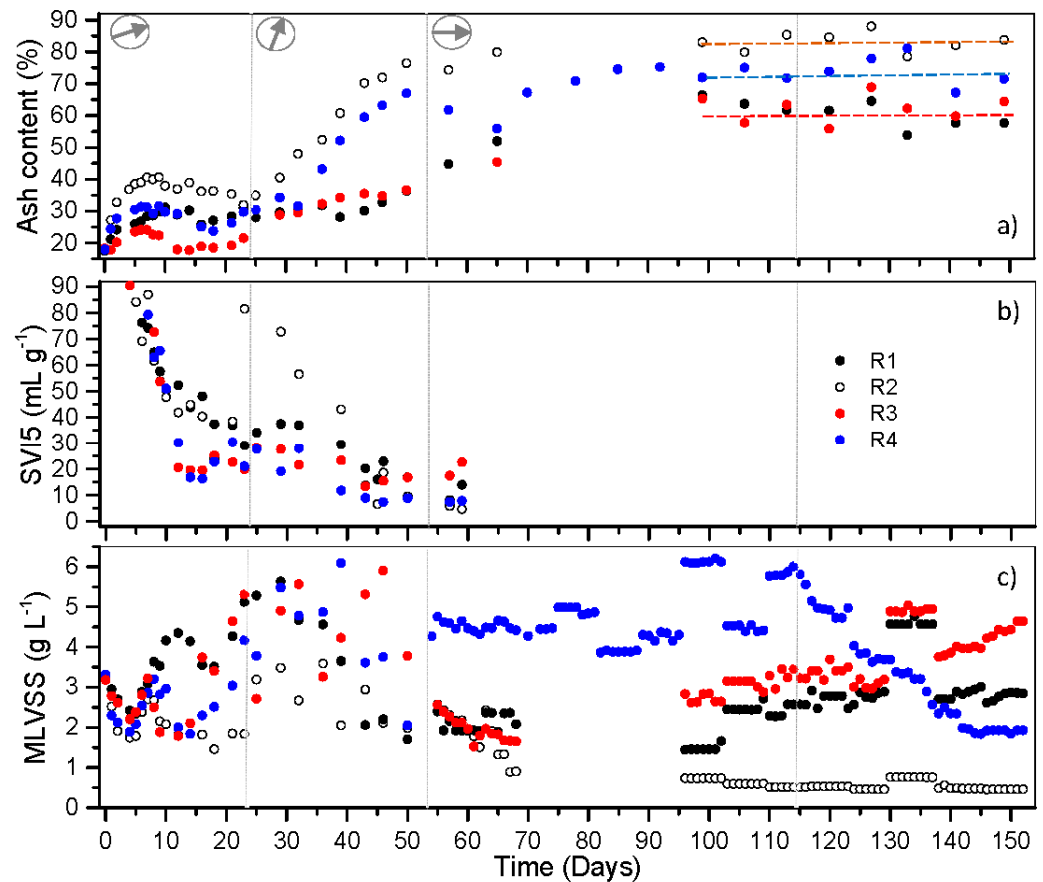


Figure 3. Profiles of ash content (a), SVI_5 (b), and MLSS-MLVSS (c) in R1 and R3 (at 21 °C), R2 and R4 (at 32 °C) over the operation time.

Based on the ash content and its increasing rate during the whole operational period, the ash content curves in Figure 3a can be divided into three distinct stages, from the early days to the stable state with granule ash content increased slightly, dramatically, and negligibly, respectively, as indicated with vertical dotted lines in Figure 3a.

Although ash content in granules showed similar changing trends, it is still very obvious that ash content increasing rates and granule ash contents in 4 reactors were different. Granule ash contents in R2 and R4 at 32 °C increased more dramatically than those in R1 and R3 at 21 °C before day 60 and then stabilized at 80% and 70%, respectively, while it took a longer time for granule ash contents in R1 and R3 at 21 °C to stabilize at 58%. Since the main difference in this phase between R1 and R3, and R2 and R4 is the temperature, it can be believed that the difference in granule ash content increasing rates and stable ash contents were mainly attributed to temperature with higher temperature in R2 and R4 benefiting quicker and more ash accumulation.

During the first 21-days, apart from the temperature difference, there was also a COD/N difference. It can be seen that granule ash content increased more quickly with COD/N of 20 in R1 than COD/N of 5 in R3 at 21 °C. A similar trend was observed with COD/N of 20 in R2 and COD/N of 5 in R4 at 32 °C. Thus, it can be seen that a higher COD/N ratio with little nitrifying activity is favorable to ash accumulation in sludge, which is probably due to a slight pH difference caused by nitrification at low COD/N ratios.

Due to a steep ash content increase in R2 at 32 °C, granule ash content reached 78% on day 50. With such high granule ash content, granule disintegration was observed and

granules broke into pieces, which resulted in a quick biomass wash-out and a very low biomass concentration (less than 0.5 g L^{-1}), as shown in Figure 3c. The influent ammonium-nitrogen concentration had to be dropped to 65 mg L^{-1} to respond to significantly reduced nitrification capacity and performance, as shown in Figure 4. R2 operation basically collapsed, although we still maintained its operation. At $32 \text{ }^\circ\text{C}$, since granule ash content increasing rate and ash content at stable state in R4 was slightly lower than R2, probably due to the low COD/N ratio in Phase 1, R4 maintained stable operation for more than 110 days with stable biomass concentration at $5\text{--}6 \text{ g L}^{-1}$; however, granule disintegration was observed after day 110, which led to the biomass washout and reduced biomass concentration, as shown in Figure 3c. Both R2 and R4 at $32 \text{ }^\circ\text{C}$ experienced granule disintegration, which should not be a coincidence. For R1 and R3 at $21 \text{ }^\circ\text{C}$, nitrifying biomass concentrations were stable until the end of operation after 153 days, and ash contents were at around 58%. By comparing two different temperatures and ash contents, it can be seen that higher temperatures resulted in higher ash contents, which might lead to the instability of nitrifying granules in the short term or long term. The stability of granules with high ash contents is seldom studied. However, Xue et al. [29] observed the deteriorated settling velocity of anammox-HAP granules, sludge bulking, and flotation when ash content was as high as 80%, an ash content close to those in R2 and R4 at $32 \text{ }^\circ\text{C}$ with instability in this study.

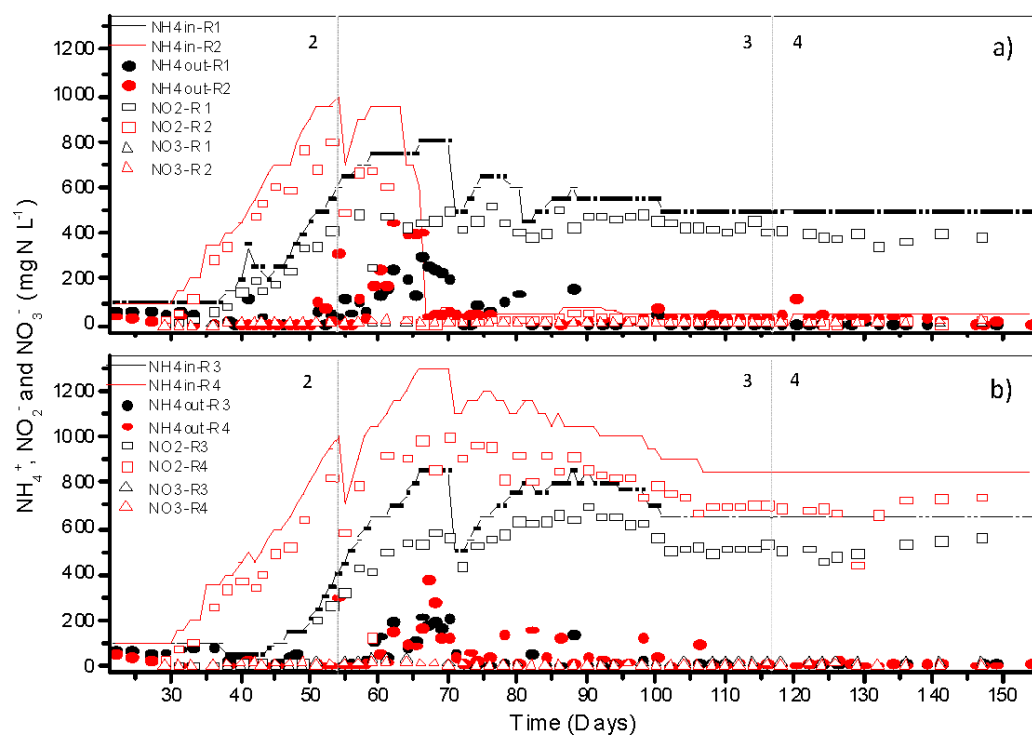


Figure 4. Profiles of nitrogen species over the time during phases 2–4, with COD reduced quickly to 0, and $\text{NH}_4^+\text{-N}$ increased to certain values in R1 and R3 at $21 \text{ }^\circ\text{C}$ (a), and R2 and R4 at $32 \text{ }^\circ\text{C}$ (b).

3.3. Performance of Nitrifying Granules at Different Temperatures and Their Specific Ammonium Oxidation Activities

On day 21, all sludge in 4 reactors was almost pure granules. From day 22, the influent $\text{NH}_4^+\text{-N}$ concentration was increased step-wise, alongside the concurrent decrease in COD concentration to transform newly formed heterotrophic granules to nitrifying granules, as shown in Figure 4. By the end of phase 2 (Table 1), heterotrophic granules were completely transformed into autotrophic nitrifying granules with the higher influent ammonium increasing rates in R2 and R4 at $32 \text{ }^\circ\text{C}$ than R1 and R3 at $21 \text{ }^\circ\text{C}$. Meanwhile, by comparing R1 and R3, and R2 and R4 with two different COD/N ratios at the same temperatures, it was found that initial low COD/N ratio and high ammonium concentra-

tion did not help the enrichment rate of nitrifying bacteria in granules. It is well known that the nitrifying bacteria growth rate is higher at a higher temperature than a lower temperature. From the results in this study, it looks as if the enrichment of nitrifying bacteria in heterotrophic granules was highly dependent on temperature instead of initial ammonium concentrations in the influent. However, the maximum influent ammonium concentration reached 1300 mg N L^{-1} in R4 with the initial COD/N ratio of 5 in phase 1, higher than 1000 mg N L^{-1} in R2 with the initial COD/N ratio of 20 in phase 1 at 32°C . Similar results were obtained at 21°C in R3 (850 mg N L^{-1}) as shown in Figure 4b and R1 (800 mg N L^{-1}) as shown in Figure 4a. These results suggest that higher initial ammonium concentration might be conducive to the enrichment of nitrifying bacteria that are capable of withstanding higher free ammonia concentrations and, thus, can treat higher influent ammonium concentration. During the whole operation period at 21°C , the influent ammonium concentration in R3 was always higher than that in R1, indicating further that higher initial ammonium concentration in phase 1 was beneficial for the tolerance of nitrifying granules to high ammonium concentration in the long run.

It was observed, however, that ammonium removal efficiencies in all reactors dropped after they reached the maximum influent ammonium concentrations which had to be reduced to ensure more than 90% ammonium removal efficiencies. R2 collapsed completely due to granule disintegration and biomass wash-out. The free ammonia (FA) concentrations, as shown in Figure S1, increased quickly and reached close to 180 mg N L^{-1} in R2 and R4 at 32°C and 80 mg N L^{-1} in R1 and R3 at 21°C , which were higher or close to the maximum FA concentration that AOB could tolerate [30]. The inhibition from FA might be one of the main reasons that nitrifying granules could not deal with the maximum influent ammonium concentration applied to reactors, i.e., 800, 1000, 850, 1300 mg N L^{-1} , for the long run.

Furthermore, it was found from Figure 5 that specific ammonium oxidization rates of nitrifying granules in all reactors dropped from day 58 to day 121, suggesting reduced nitrifying activities. During this period, ash content increased in nitrifying granules, as shown in Figure 3. This phenomenon in nitrifying granules is similar to that reported by Liu et al. [7] that the increased ash content in heterotrophic granules led to reduced microbial activities. Meanwhile, it could be seen from Figure 5 that the specific ammonium oxidization rates of nitrifying granules in R4 at 32°C were lower than those in R1 and R3 at 21°C , which is contradictory to the common report that nitrifying bacteria had a higher nitrification rate at a higher temperature. For example, it was reported that a temperature increment at 20°C resulted in a nitrification rate increase of 4.275% per $^\circ\text{C}$ by nitrifying biofilm [31]. Therefore, the most reasonable explanation is that the higher ash content in R4 at 32°C resulted in the reduced specific ammonium oxidization rate. The reduced microbial activities with the accumulation of inorganics in granules were reported in other studies with other types of granules, as well [15,16,32].

In all 4 reactors, ammonium was mainly oxidized to nitrite with negligible nitrate production (less than 10 mg L^{-1}), and the stable nitritation was maintained during the whole operation period without special controls. High influent ammonium concentration to around 1000 mg L^{-1} might not be the reason for partial nitrification because Chen et al. [28] reported complete nitrification with similar influent ammonium concentration and operational conditions, except for lower calcium concentration and lower ash content. Poot et al. [33] found that the control of the residual ammonium concentration had proven to be effective for repression of *Nitrospira* spp. at 20°C , and the stratification of an outer AOB layer in the granule structure was found to be highly important to maintain stable partial nitritation in the long term. Thus, it is speculated that relatively high residual ammonium concentration (10 mg N L^{-1}) and high ash content in granules contributed to the maintenance of stable nitritation by increasing mass transfer resistance in granules with ammonium oxidizing bacteria grown in the outer layer of granules.

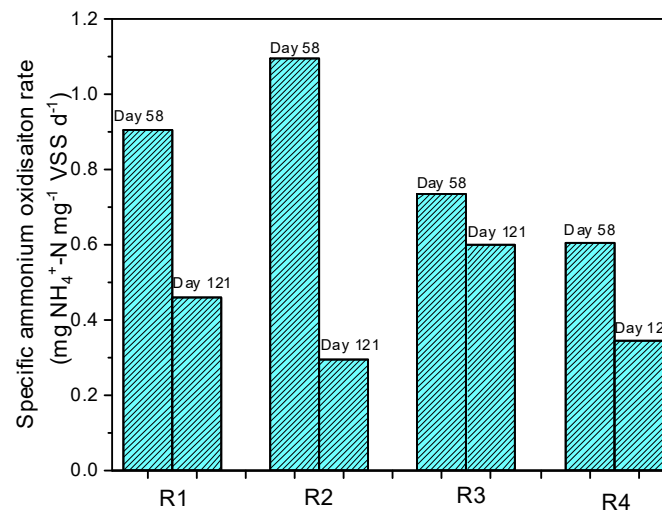


Figure 5. Specific ammonium oxidizing rates of nitrifying granules in 4 reactors on operational days of 58 and 121.

Within 37 days, heterotrophic granules were completely transformed into partial nitrifying granules to treat nitrogen-rich wastewater with influent $\text{NH}_4^+\text{-N}$ concentration as high as 950 mg L^{-1} at 32°C and 650 mg L^{-1} at 21°C . Similar results were also reported by Chen et al. [5], where nitrifying granules could treat $1000 \text{ mg NH}_4^+\text{-N L}^{-1}$ in less than 55 days from reactor start-up by activated sludge. However, nitrifying sludge was inoculated in their reactors, while activated sludge without nitrification capability was inoculated in our study. The strategy used in this study to form heterotrophic granules rapidly first and then to transform heterotrophic granules to nitrifying granules resulted in the quicker formation of partial nitrifying granules, compared with 70 and 146 days reported in other studies [34–36].

3.4. Calcium Precipitation and Accumulation in Partial Nitrifying Granules at Moderate and High Temperatures

To understand the mineral accumulation in nitrifying granules, metal elements and phosphorus in granules from R3 at 21°C and R4 at 32°C were analyzed and shown in Table 2. It can be seen that the inorganic elements contributing to accumulated ash in granules are mainly phosphorus and calcium, with calcium contents up to 17–25% and phosphorus contents up to 4.1–7.7%. According to Table 2, calcium concentration in tap water was 102 mg L^{-1} due to chalk aquifer in Southampton, UK. This hard water is one of the main reasons for the excessive precipitation and accumulation of calcium precipitates in nitrifying granules. Ca/P molar ratio in granules from R3 was 1.74, which is very close to the Ca/P ratio of pure hydroxyapatite (i.e., 1.67). XRD analysis results shown in Figure S2 proved that the main inorganic precipitate in granules from R3 was hydroxyapatite. Based on phosphorus content in Table 2, the calculated hydroxyapatite content of granules in R3 would be 42%, close to the actual ash content of 55%, as shown in Figure 3. Ca/P molar ratio in granules from R4, however, was much higher than 1.67, which reached 4.83. XRD analysis showed the presence of both hydroxyapatite and calcite. Based on the phosphorus content of granules in R4, the calculated hydroxyapatite content was 22%, and, based on calcium content after deducting calcium in hydroxyapatite, the calculated calcite was 42%, resulting in a total ash content of 64%, close to the actual ash content of 73% in Figure 3. The small percentage difference between calculated ash content and actual ash content might be due to a small percentage of other types of amorphous calcium precipitates, which might not yet convert to crystals. It is very interesting to note that higher temperature did not only promote more mineral precipitation and accumulation in granules but also stimulated co-precipitation and accumulation of hydroxyapatite and calcite.

Table 2. The contents of main metal elements and phosphorus in granules from R3 at 21 °C and R4 at 32 °C on day 107 at the end of phase 3.

	Unit	Na	Mg	P	K	Ca	Fe	Ca/P
R3	mg g ⁻¹ TSS	12.79	0.59	76.80	0.94	172.30	2.94	1.74
R4	mg g ⁻¹ TSS	11.42	0.91	40.86	0.36	254.40	3.05	4.82
Tap water	mg L ⁻¹	13.95	2.18	0.10	1.70	102.70	0.027	
Feedstock elements	mg L ⁻¹	7210.00–3285.71	4.15	15.20	19.28	110.46	2.00	5.63

A typical P content in activated sludge is usually less than 1% [37], but, in this study, P content in granules from R3 and R4 reached 7.7% and 4.1%, respectively, which are comparable to the phosphorus content in sewage sludge incineration ash ranging between 4 and 9% [38]. Thus, hydroxyapatite precipitation and accumulation in nitrifying granules could be beneficial for phosphorus removal and recovery. From this perspective, the moderate temperature is more beneficial because hydroxyapatite would be more dominant with a higher phosphorus content at moderate temperature compared with high temperature.

EDX was then conducted to observe the distribution of calcium precipitates on the granule surface and cores by halving granules. It can be seen from Figure 6 that, for granules in both R3 and R4, calcium phosphate and other calcium precipitates were mainly located in the cores of granules, while there were no calcium precipitates on the granule surface. Thus, it is less likely for calcium precipitate to form in bulk liquid and then deposit on the granule surface. The similar element distribution was previously described for both heterotrophic aerobic granules [12] and EBPR granules with 30–35% of ash contents by other researchers [13], who reported that external layers of granules were mainly composed of microorganisms with high contents of C, N, and O, whereas inorganic contents, such as Ca and P, were much higher toward the core of the particles.

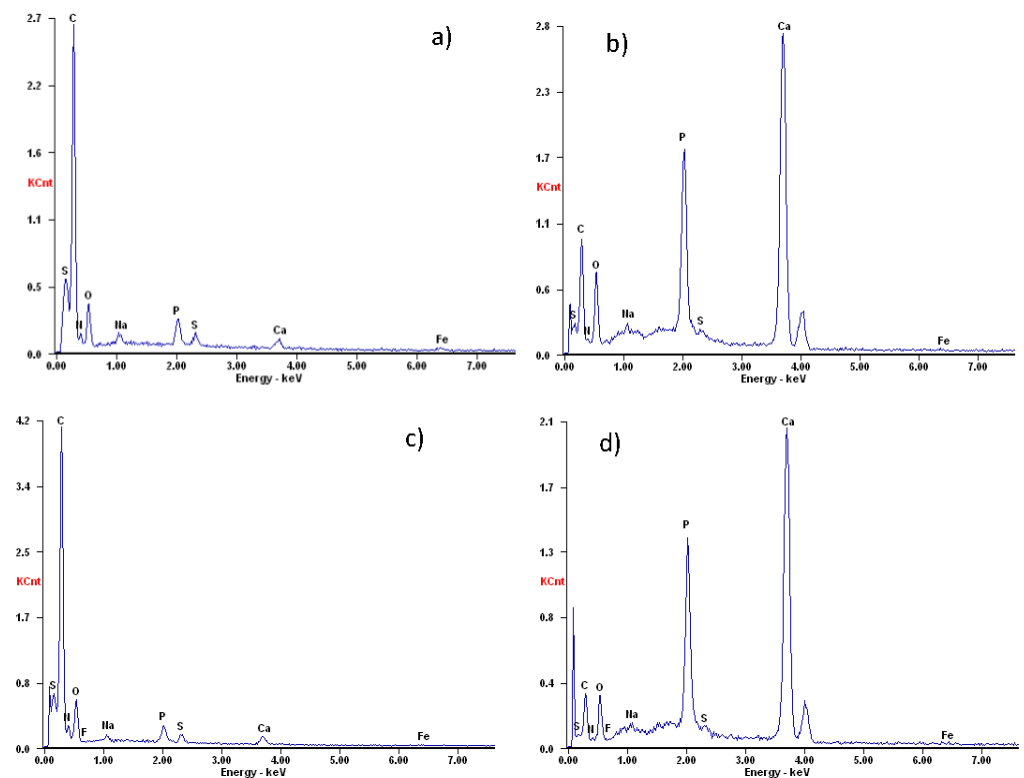


Figure 6. Elemental composition of the (a) surface and (b) core of granules in R3 and (c) surface and (d) core of granules in R4 by EDX analysis.

There are two assumptions to explain this phenomenon. One is that inorganic precipitates form in the wastewater first, which then act as carriers for bacteria to attach and form granules [11]. The other possibility is that granule structure and high EPS content in granules could provide favorable micro-environment for biomineralization due to microbial activity, causing biologically induced mineral precipitation in granules [3,13]. It is less likely that mineral precipitation in granules is species-specific, but potential bacteria associated with precipitation of calcium carbonate and calcium phosphate were detected in granular sludge in the co-precipitated calcite and hydroxyapatite [39]. No matter which assumption is tenable, the bacteria tend to grow on the granule surface due to easy access to nutrients and oxygen in water with less mass transfer resistance.

4. Conclusions

Mineral precipitation and accumulation in nitrifying granules were investigated with hard water and two different temperatures, i.e., the moderate temperature at 21 °C and the high temperature at 32 °C. The key findings were summarized as below:

- Initial ammonium concentration and temperature from moderate 21 °C to 32 °C had negligible effects on the speed of heterotrophic granules.
- Mature granules had much higher calcium precipitates accumulated inside compared with newly formed granules, and suspended sludge, indicating the importance of long sludge retention time for the accumulation of calcium precipitates.
- Higher temperature promoted more mineral precipitates in granules, in general. Specifically, high temperature promoted co-precipitation and accumulation of hydroxyapatite and calcite, while moderate temperature was more beneficial for the dominance of hydroxyapatite in granules.
- Increased calcium precipitates in nitrifying granules resulted in reduced microbial activities.
- High mineral content in granules led to the instability of nitrifying granules at a higher temperature in the short or long run.

Overall, mature granules have much higher calcium precipitate contents than young granules due to the long retention time. The temperature has significant effects on calcium precipitation, precipitate species, ash accumulation, ash content, microbial activity, and long-term stability when ash content is high.

Supplementary Materials: The following are available online at <https://www.mdpi.com/article/10.3390/pr9101710/s1>, Figure S1: Concentrations of free ammonia (FA) (a) and free nitrous acid (FNA) (b) over the operation time with the increased influent NH₄⁺-N concentration. Figure S2: The inorganic solid phases present within granules from R3 and R4 on day 121 by XRD analysis.

Author Contributions: Conceptualization, Y.-Q.L.; formal analysis, S.C.; investigation, S.C.; writing—original draft preparation, S.C. and Y.-Q.L.; writing—review and editing, Y.-Q.L.; supervision, Y.-Q.L. All authors have read and agreed to the published version of the manuscript.

Funding: This research received no external funding, and the APC was funded by EBNet, BBSRC, UK.

Institutional Review Board Statement: Not applicable.

Informed Consent Statement: Not applicable.

Data Availability Statement: Not applicable.

Conflicts of Interest: The authors declare no conflict of interest.

References

1. Fukuzaki, S.; Nishio, N.; Sakurai, H.; Nagai, S. Characteristics of methanogenic granules grown on propionate in an upflow anaerobic sludge blanket (UASB) reactor. *J. Ferment. Bioeng.* **1991**, *71*, 50–57. [[CrossRef](#)]
2. Johansson, S.; Rusalleda, M.; Colprim, J. Phosphorus recovery through biologically induced precipitation by partial nitrification-anammox granular biomass. *Chem. Eng. J.* **2017**, *327*, 881–888. [[CrossRef](#)]

3. de Kreuk, M.; Heijnen, J.; van Loosdrecht, M. Simultaneous COD, nitrogen, and phosphate removal by aerobic granular sludge. *Biotechnol. Bioeng.* **2005**, *90*, 761–769. [[CrossRef](#)]
4. Liu, Y.-Q.; Lan, G.-H.; Zeng, P. Size-dependent calcium carbonate precipitation induced microbiologically in aerobic granules. *Chem. Eng. J.* **2016**, *285*, 341–348. [[CrossRef](#)]
5. Lin, Y.; Lotti, T.; Sharma, P.; van Loosdrecht, M. Apatite accumulation enhances the mechanical property of anammox granules. *Water Res.* **2013**, *47*, 4556–4566. [[CrossRef](#)] [[PubMed](#)]
6. Juang, Y.-C.; Adav, S.S.; Lee, D.-J.; Tay, J.-H. Stable aerobic granules for continuous-flow reactors: Precipitating calcium and iron salts in granular interiors. *Bioresour. Technol.* **2010**, *101*, 8051–8057. [[CrossRef](#)] [[PubMed](#)]
7. Liu, Y.-Q.; Lan, G.-H.; Zeng, P. Excessive precipitation of CaCO₃ as aragonite in a continuous aerobic granular sludge reactor. *Appl. Microbiol. Biotechnol.* **2015**, *99*, 8225–8234. [[CrossRef](#)] [[PubMed](#)]
8. Jiang, H.-L.; Tay, J.-H.; Liu, Y.; Tay, S.T.-L. Ca²⁺ augmentation for enhancement of aerobically grown microbial granules in sludge blanket reactors. *Biotechnol. Lett.* **2003**, *25*, 95–99. [[CrossRef](#)] [[PubMed](#)]
9. Wang, S.; Shi, W.; Yu, S.; Yi, X.; Yang, X. Formation of aerobic granules by Mg²⁺ and Al³⁺ augmentation in sequencing batch airlift reactor at low temperature. *Bioprocess Biosyst. Eng.* **2012**, *35*, 1049–1055. [[CrossRef](#)] [[PubMed](#)]
10. Yilmaz, G.; Bozkurt, U.; Magden, K.A. Effect of iron ions (Fe²⁺, Fe³⁺) on the formation and structure of aerobic granular sludge. *Biodegradation* **2017**, *28*, 53–68. [[CrossRef](#)]
11. Ma, H.; Xue, Y.; Zhang, Y.; Kobayashi, T.; Kubota, K.; Li, Y.-Y. Simultaneous nitrogen removal and phosphorus recovery using an anammox expanded reactor operated at 25° C. *Water Res.* **2020**, *172*, 115510. [[CrossRef](#)] [[PubMed](#)]
12. Ren, T.-T.; Liu, L.; Sheng, G.-P.; Liu, X.-W.; Yu, H.-Q.; Zhang, M.-C.; Zhu, J.-R. Calcium spatial distribution in aerobic granules and its effects on granule structure, strength and bioactivity. *Water Res.* **2008**, *42*, 3343–3352. [[CrossRef](#)] [[PubMed](#)]
13. Mañas, A.; Biscans, B.; Sperandio, M. Biologically induced phosphorus precipitation in aerobic granular sludge process. *Water Res.* **2011**, *45*, 3776–3786. [[CrossRef](#)]
14. Yu, T.; Tian, L.; You, X.; Wang, L.; Zhao, S.; Kang, D.; Xu, D.; Zeng, Z.; Zhang, M.; Zheng, P. Deactivation mechanism of calcified anaerobic granule: Space occupation and pore blockage. *Water Res.* **2019**, *166*, 115062. [[CrossRef](#)] [[PubMed](#)]
15. Feldman, H.; Alsina, X.F.; Ramin, P.; Kjellberg, K.; Jeppsson, U.; Batstone, D.J.; Gernaey, K.V. Assessing the effects of intra-granule precipitation in a full-scale industrial anaerobic digester. *Water Sci. Technol.* **2019**, *79*, 1327–1337. [[CrossRef](#)] [[PubMed](#)]
16. Van Langerak, E.; Ramaekers, H.; Wiechers, J.; Veeken, A.; Hamelers, H.; Lettinga, G. Impact of location of CaCO₃ precipitation on the development of intact anaerobic sludge. *Water Res.* **2000**, *34*, 437–446. [[CrossRef](#)]
17. de Kreuk, M.; Pronk, M.; van Loosdrecht, M. Formation of aerobic granules and conversion processes in an aerobic granular sludge reactor at moderate and low temperatures. *Water Res.* **2005**, *39*, 4476–4484. [[CrossRef](#)]
18. Ab Halim, M.H.; Anuar, A.N.; Jamal, N.S.A.; Azmi, S.I.; Ujang, Z.; Bob, M.M. Influence of high temperature on the performance of aerobic granular sludge in biological treatment of wastewater. *J. Environ. Manag.* **2016**, *184*, 271–280. [[CrossRef](#)]
19. APHA. *Standard Methods of Water and Wastewater*, 22nd ed.; American Public Health Association, American Water Works Association, Water Environment Federation: Washington, DC, USA, 2012.
20. Liu, Y.Q.; Kong, Y.H.; Zhang, R.; Zhang, X.; Wong, F.S.; Tay, J.H.; Zhu, J.R.; Jiang, W.J.; Liu, W.-T. Microbial population dynamics of granular aerobic sequencing batch reactors during start-up and steady state periods. *Water Sci. Technol.* **2010**, *62*, 1281–1287. [[CrossRef](#)]
21. Beun, J.; Hendriks, A.; van Loosdrecht, M.; Morgenroth, E.; Wilderer, P.; Heijnen, J. Aerobic granulation in a sequencing batch reactor. *Water Res.* **1999**, *33*, 2283–2290. [[CrossRef](#)]
22. BSI. BS 6068-2.11:1984, ISO 7150-1:1984 *Water Quality. Physical, Chemical and Biochemical Methods. Determination of Ammonium: Manual Spectrometric Method*; British Standards Institution: London, UK, 1984.
23. Liu, Y.-Q.; Moy, B.; Kong, Y.-H.; Tay, J.-H. Formation, physical characteristics and microbial community structure of aerobic granules in a pilot-scale sequencing batch reactor for real wastewater treatment. *Enzym. Microb. Technol.* **2010**, *46*, 520–525. [[CrossRef](#)] [[PubMed](#)]
24. Liu, Y.-Q.; Kong, Y.; Tay, J.-H.; Zhu, J. Enhancement of start-up of pilot-scale granular SBR fed with real wastewater. *Sep. Purif. Technol.* **2011**, *82*, 190–196. [[CrossRef](#)]
25. Liu, Y.-Q.; Tay, J.-H. Characteristics and stability of aerobic granules cultivated with different starvation time. *Appl. Microbiol. Biotechnol.* **2007**, *75*, 205–210. [[CrossRef](#)] [[PubMed](#)]
26. Yang, S.-F.; Tay, J.-H.; Liu, Y. Inhibition of free ammonia to the formation of aerobic granules. *Biochem. Eng. J.* **2004**, *17*, 41–48. [[CrossRef](#)]
27. Liu, Y.-Q.; Tay, J.-H. Fast formation of aerobic granules by combining strong hydraulic selection pressure with over-stressed organic loading rate. *Water Res.* **2015**, *80*, 256–266. [[CrossRef](#)]
28. Chen, F.-Y.; Liu, Y.-Q.; Tay, J.-H.; Ning, P. Rapid formation of nitrifying granules treating high-strength ammonium wastewater in a sequencing batch reactor. *Appl. Microbiol. Biotechnol.* **2015**, *99*, 4445–4452. [[CrossRef](#)]
29. Xue, Y.; Ma, H.; Kong, Z.; Guo, Y.; Li, Y.-Y. Bulking and floatation of the anammox-HAP granule caused by low phosphate concentration in the anammox reactor of expanded granular sludge bed (EGSB). *Bioresour. Technol.* **2020**, *310*, 123421. [[CrossRef](#)]
30. Anthonisen, A.C.; Loehr, R.C.; Prakasam, T.B.S.; Srinath, E.G. Inhibition of Nitrification by Ammonia and Nitrous Acid. *J. Water Pollut. Control. Fed.* **1976**, *48*, 835–852.
31. Zhu, S.; Chen, S. The impact of temperature on nitrification rate in fixed film biofilters. *Aquac. Eng.* **2002**, *26*, 221–237. [[CrossRef](#)]

32. Xing, B.-S.; Guo, Q.; Yang, G.-F.; Zhang, Z.-Z.; Li, P.; Guo, L.-X.; Jin, R.-C. The properties of anaerobic ammonium oxidation (anammox) granules: Roles of ambient temperature, salinity and calcium concentration. *Sep. Purif. Technol.* **2015**, *147*, 311–318. [[CrossRef](#)]
33. Poot, V.; Hoekstra, M.; Geleijnse, M.A.; van Loosdrecht, M.C.; Pérez, J. Effects of the residual ammonium concentration on NOB repression during partial nitrification with granular sludge. *Water Res.* **2016**, *106*, 518–530. [[CrossRef](#)]
34. Kim, D.-J.; Seo, D. Selective enrichment and granulation of ammonia oxidizers in a sequencing batch airlift reactor. *Process. Biochem.* **2006**, *41*, 1055–1062. [[CrossRef](#)]
35. Song, Y.; Ishii, S.; Rathnayak, L.; Ito, T.; Satoh, H.; Okabe, S. Development and characterization of the partial nitrification aerobic granules in a sequencing batch airlift reactor. *Bioresour. Technol.* **2013**, *139*, 285–291. [[CrossRef](#)]
36. Wei, D.; Xue, X.; Yan, L.-G.; Sun, M.; Zhang, G.; Shi, L.; Du, B. Effect of influent ammonium concentration on the shift of full nitrification to partial nitrification in a sequencing batch reactor at ambient temperature. *Chem. Eng. J.* **2014**, *235*, 19–26. [[CrossRef](#)]
37. Metcalf, E. *Wastewater Engineering: Treatment, Disposal and Reuse*; McGraw-Hill Inc.: New York, NY, USA, 2003.
38. Franz, M. Phosphate fertilizer from sewage sludge ash (SSA). *Waste Manag.* **2008**, *28*, 1809–1818. [[CrossRef](#)] [[PubMed](#)]
39. Gonzalez-Martinez, A.; Rodriguez-Sanchez, A.; Rivadeneyra, M.A.; Rivadeneyra, A.; Martin-Ramos, D.; Vahala, R.; Gonzalez-Lopez, J. 16S rRNA gene-based characterization of bacteria potentially associated with phosphate and carbonate precipitation from a granular autotrophic nitrogen removal bioreactor. *Appl. Microbiol. Biotechnol.* **2016**, *101*, 817–829. [[CrossRef](#)] [[PubMed](#)]